# Colossal magnetoresistance and hyperfine interactions in iron-doped $La_{0.75}Ca_{0.25}MnO_3$

B. Hannoyer
*Laboratoire d'Analyse Spectroscopique et de Traitement de Surface des Matériaux, Université de Rouen, 76821 Mont-Saint-Aignan Cedex, France*

G. Marest*
*Institut de Physique Nucléaire de Lyon, IN2P3 et Université Lyon I, 43 Boulevard du 11 Novembre 1918, 69622 Villeurbanne Cedex, France*

J. M. Greneche
*Laboratoire de Physique de l'Etat Condensé, UPRESA CNRS 6087 Université du Maine, 72 085 Le Mans Cedex 9, France*

Ravi Bathe and S. I. Patil
*Center for Advanced Studies in Materials Science and Solid State Physics, Department of Physics, University of Poona, Pune 411 007, India*

S. B. Ogale
*NSF-MRSEC on Oxides, Surfaces and Probes, Departments of Physics and Materials Science, University of Maryland, College Park, Maryland 20742*

(Received 29 July 1999; revised manuscript received 1 December 1999)

Detailed measurements and analysis of hyperfine properties of iron-doped $La_{0.75}Ca_{0.25}Mn_{1-x}Fe_xO_3$ are reported. In a previous paper [Phys. Rev. B **57**, 7841 (1998)] it was shown that a very small increase of $x$ from 0.0425 to 0.045 causes dramatic changes in the transport properties, whereas no changes are detected either in the structural phase or the Mössbauer data. In the present study a complete analysis of Mössbauer data registered in the temperature range of 300–4 K is presented. From 300 K down to 190 K the samples are in a paramagnetic state. Below 190 K a magnetic order begins to develop, although a paramagnetic contribution persists down to 77 K. This existence of paramagneticlike domains deep into the so-called ferromagnetic metallic regime provides evidence of the two-phase character of the metallic state in the mixed-valent manganite system. The quadrupole splitting of the major spectral component shows a jump at the para-ferro transition. This reflects lowering of the local point-charge symmetry in the remaining paramagneticlike phase in the ferromagnetic regime, presumably because of the changes in its shape function or its character, as the ferromagnetic clusters stabilize in space. Another small component of the spectrum, which appears to represent the grain-boundary region, exhibits ferromagnetic ordering at around 100 K and also a behavior opposite to that of the major fraction under external magnetic field.

## I. INTRODUCTION

Interest in the transport and magnetic properties of oxide perovskite systems belonging to the $A_{1-x}B_xMnO_{3+y}$ ($A$ = La, Nd, Y; $B$ = Ca, Ba, Sr) family has grown rather sharply during the past few years since the discovery of ''colossal magnetoresistance'' (CMR) in such ($x \sim 0.33$) compounds.[1–4] Relatively recent interesting observations dealing with charge ordering and stripe formation[5] and orbital ordering,[6] as well as the suggestions of two-phase models[7–8] and percolative transport,[7–8,9] have enhanced the activity in this field even further.

Different explanations of the CMR mechanism have been proposed, but the role of $Mn^{3+}$-O-$Mn^{4+}$ superexchange in the magnetic properties of Mn based perovskites remains to be fully understood.[10–13] Thus introduction of perturbations into the magnetic Mn lattice sites themselves appears to be a promising approach for fruitful investigations. Only a few studies have been conducted thus far on doping at the Mn sites, which are at the heart of the double exchange. In a recent paper, Blasco *et al.*[14] have studied the effect of the substitution for Mn with Al in the magnetoresistive perovskite $La_{2/3}Ca_{1/3}MnO_3$. Al has no magnetic moment but its atomic radius is smaller than that of Mn. The substituted compounds were found to be magnetically inhomogeneous because of the introduction of a structural disorder and the formation of oxygen vacancies in the lattice. At low temperatures, coexistence of regions with very different magnetic coherence lengths was found. The replacement of $Mn^{3+}$ by $Fe^{3+}$ presents a great interest because of their compatible ionic sizes and their different magnetic moments. Recently, it has been shown that the the lattice parameter is essentially unchanged by iron substitution.[15–16] However, Righi *et al.* think that the presence of $Fe^{3+}$ produces distortions (change in the Mn-O distances and in the Mn-O-Mn angles) which are not detected in x-ray-diffraction pattern.[16] The CMR was dramatically enhanced for 12% Mn replaced by Fe.[15] The effect of Fe doping was explained in terms of the changes in band structure as doping with Fe causes a depletion of the $Mn^{3+}/Mn^{4+}$ ratio, the population of the hop-

 

ping electrons and the number of available hopping sites.[15] Thus the double exchange is suppressed, resulting in the reduction of ferromagnetism and metallic conduction.

To our knowledge, only one Mössbauer study of iron-doped $La_{0.75}Ca_{0.25}MnO_3$ (LCMO) has been performed to probe the magnetic effects induced after a light substitution of $^{57}Fe$ (2%) for Mn.[17] In the said work, the Mössbauer spectrum consisted of a single doublet at room temperature and, at the Curie temperature ($T_c = 210$ K), part of the spectrum was magnetically split. The area of this part increased with the lowering of the temperature. At 150 K an increase of the quadrupolar splitting of the doublet was noted, and was explained by a possible structural transformation of the matrix. Finally, at liquid-helium temperature, the spectrum displayed a single magnetic sextet. The evolution of the Mössbauer spectrum as a function of temperature was attributed to the existence of ferromagnetic clusters with a size distribution. The same research group has recently interpreted the temperature evolution of the Mössbauer spectrum obtained for a $La_{0.67}Ca_{0.33}Mn_{0.99}Fe_{0.01}O_3$ sample using a model based on an antiferromagnetic impurity in a ferromagnetic host.[18]

In a preceeding paper, we have examined the transport properties for iron substitution ''*x*'' in the range 0–5% of Mn.[19] In accordance with results reported previously[20–24] the undoped sample undergoes an insulator to metal transition at $T_p = 240$ K, the peak temperature. The sample resistivity was found to increase with iron doping, relatively slowly up to $x = 0.0425$, but dramatic changes occurred in the transport properties when *x* was increased from 0.0425 to 0.045. The peak resistivity $T_p$ decreased sharply from 167 to 88 K whereas no structural phase change was detected by x-ray-diffraction analysis. No change was observed in magnetization as well. Our conclusion was that at a critical dopant concentration (when the average Fe-Fe separation is smaller than three lattice units), a localization-delocalization-type transition occurs for the quasiparticles (possibly magnetic polarons) as introduced by Hundley *et al.* and Jaime *et al.*[20]

In the present study, we report a complete analysis of the Mössbauer spectra registered for $x = 0.0425$ and 0.045 in the temperature range 300–4 K. Note that the Fe concentration examined here is near the threshold of the localization-delocalization transition, as against the work of Pissas *et al.*[17] where it was much below this threshold.

## II. EXPERIMENT

Ceramic samples of $La_{0.75}Ca_{0.25}Mn_{1-x}Fe_xO_3$ with *x* varying in the range 0–0.05 were prepared by the standard ceramic route. Stoichiometric proportions of $La_2O_3$, $CaCO_3$, $MnO_2$, and $Fe_2O_3$ with 99.999% purity were mixed, heated in air at 1223 K for 12 h, and then sintered at 1573 K for more than 20 h. In the case of the $x = 0.0425$ and 0.045 powdered samples examined by Mössbauer spectrometry, about 25% of the $Fe_2O_3$ powder used for Fe doping was enriched in $^{57}Fe$, the Mössbauer isotope, to enhance the Mössbauer signal. The resistivity measurements were carried out using four-probe method. For magnetoresistance measurements a maximum applied field of 1 T was used.

Mössbauer spectra were recorded in transmission geometry using $^{57}Co(Rh)$ source in a constant acceleration mode at different temperatures from 300 K down to 4.2 K. The velocity scale and all the data are referred to metallic $\alpha$-Fe absorber at room temperature. The spectra were analyzed by means of least-square Mosfit program in which discrete hyperfine field distributions are considered.[25] Mössbauer measurements under applied external field parallel to the $\gamma$ radiation were performed using a cryomagnetic device.

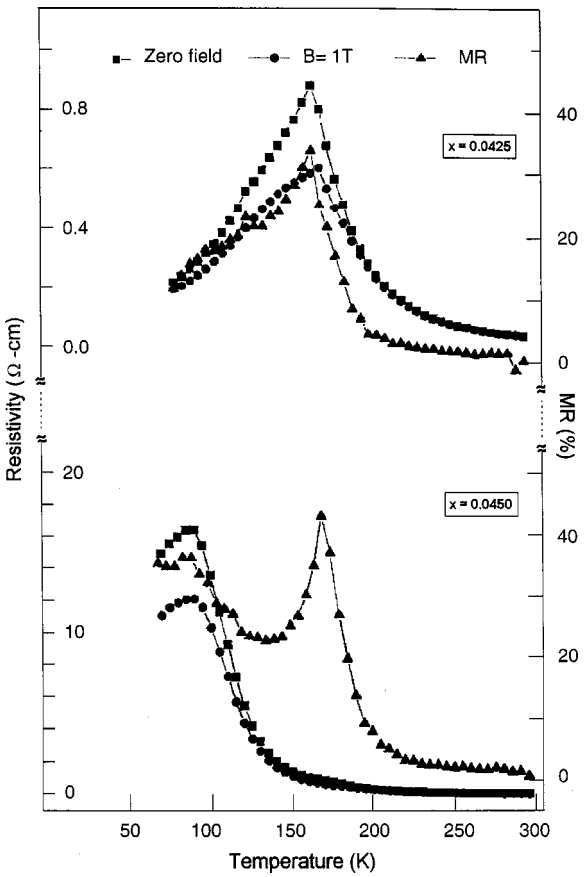


FIG. 1. Temperature dependence of the resistivity and MR (at 1 T) of $La_{0.75}Ca_{0.25}Mn_{1-x}Fe_xO_3$ perovskite for $x = 0.0425$ and $x = 0.0450$.

## III. RESULTS

Figure 1 shows the temperature dependence of the resistivity $\rho$ and the CMR effect $[\Delta\rho/\rho = \{\rho(T,H=0) - \rho(T,H)\}/\rho(T,H=0)]$ for the LCMO samples with $x = 0.0425$ and 0.0450. The entire set of data for $0 \leqslant x \leqslant 0.05$ has appeared in our preceding paper. Between $x = 0.0425$ and 0.045 the resistivity is seen to jump by a factor of 20. Interestingly, it is also observed that the maximum of the CMR effect occurs at temperatures $T_{MR}$ which are lower than the resistivity peak temperatures $T_p$ when $x \leqslant 4.25\%$, but higher when $x \geqslant 4.5\%$. As Fe is doped in the sample, both $T_p$ and $T_{MR}$ are systematically lowered as shown in Fig. 2. There is a net correlation between the dependence versus temperature of $T_p$ and $T_{MR}$. It is worthwhile to note that the two curves show a discontinuity when $x \geqslant 0.0425$, which could be correlated to the appearance of a second peak in the CMR curves at a fixed temperature of 170 K whatever the value of *x* above 0.045. Lowering of $T_p$ ($T_C$) signifies a weaker $Fe^{3+}$-O-$Mn^{4+}$ coupling than the $Mn^{3+}$-O-$Mn^{4+}$ coupling as

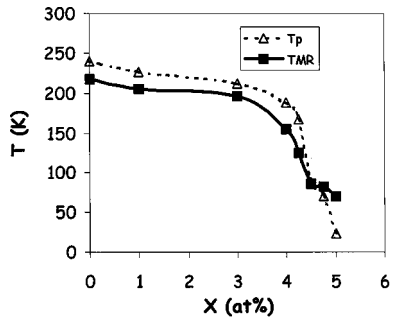


FIG. 2. Iron concentration dependence of the temperatures corresponding to the insulator-metal transition $T_p$ (△) and to the maximum of the MR effect $T_{MB}$ (■).

it has been demonstrated in spinel systems.[26]

The transmission Mössbauer spectra for the $x=0.045$ case recorded at different temperatures from 170 K down to 77 K are shown in Fig. 3. The spectra taken at 300 and 4.2 K are shown separately in Fig. 4 along with the fitted components for clarity. Since the spectra for the $x=0.0425$ case were found very similar,[19] they are not presented. From 300 K down to 190 K the samples are fully paramagnetic, and two doublets can fit the Mössbauer spectra as illustrated for the

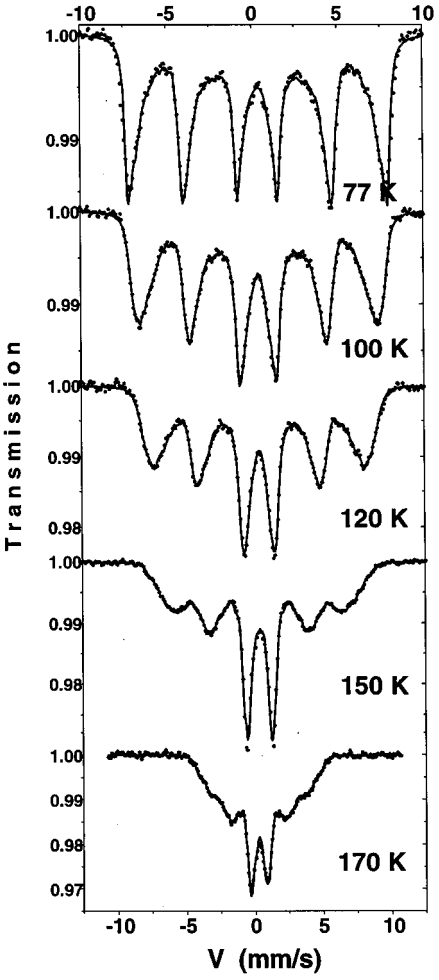


FIG. 3. Transmission Mössbauer spectra for the $La_{0.75}C_{0.25}Mn_{0.955}Fe_{0.045}O_3$ sample at different temperatures between 170 and 77 K.

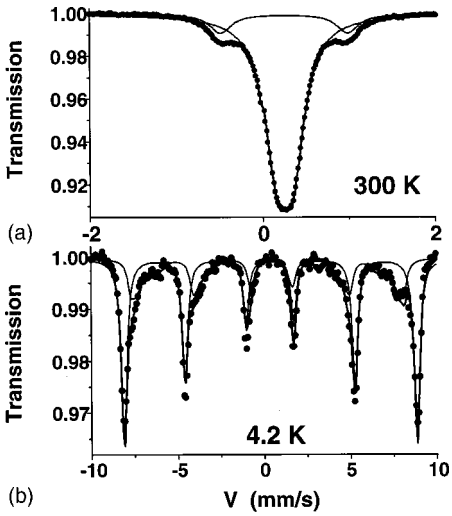


FIG. 4. Transmission Mössbauer spectra for the $La_{0.75}C_{0.25}Mn_{0.955}Fe_{0.045}O_3$ sample at (a) 300 K and (b) 4.2 K, with fitted components.

room temperature case in Fig. 4(a). At room temperature, the main doublet has hyperfine parameters (isomer shift IS $=0.35$ mm/s, quadrupolar splitting QS$=0.12$ mm/s and linewidth $\Gamma=0.32$ mm/s) which are not very different from those (IS$=0.364$ mm/s, QS$=0.176$ mm/s, $\Gamma=0.316$ mm/s) obtained by Pissas *et al.*[17] Such low QS has its origin in the orthorhombic distortion of the ideal perovskite structure. However, at variance with the cited authors, a second weak doublet with a large quadrupolar splitting (QS$=1.42$ mm/s, IS$=0.37$ mm/s, $\Gamma=0.28$ mm/s) had to be considered to obtain a good fit. This large QS reflects a very distorted site, which can have different explanations: Fe ions located in a defect structure or at the grain boundary, presence of Fe atoms with different numbers of Fe-Mn neighbors.[26] On account of the isomer shift values the charge state of iron is exclusively 3+, without coexistence of the 4+ charge state. Even when the temperature is lowered from 300 K down to 190 K the quadrupolar splitting values and the proportions of both iron sites remain temperature constant [Fig. 5(a)]. At 190 K, the appearance of broad lines makes the structure of the Mössbauer spectra complex. In the temperature range between 190 and 77 K, one observes a quadrupolar doublet-like component with broad lines superposed on a magnetic component. At lower temperatures the spectra clearly result from different magnetic components. This implies that a magnetic order begins to develop at about 190 K, yet a paramagnetic contribution remains present even down to ~77 K [Fig. 5(b)]. At 4.2 K [Fig. 4(b)] three different contributions can be distinguished in the spectrum. The most populated subspectrum (60%) has an isomer shift equal to 0.50 mm/s and a hyperfine magnetic field $B$ of 53(1) T. The second sextet with a nearly identical isomer shift (0.46 mm/s) has a lower hyperfine field $B=49(1)$ T. The remaining contribution to the spectrum (10%) consists of a distribution of magnetic fields ($\langle B\rangle=44(2)$ T). Our spectrum significantly differs from the one published by Pissas *et al.*[17] The latter only comprised of one sextet with sharp lines with $B=53.3$ T, which agrees fairly well with the main component of our spectrum. In Ref. 18, the same authors have detected two components: a well defined sextet with $B=53$ T representing

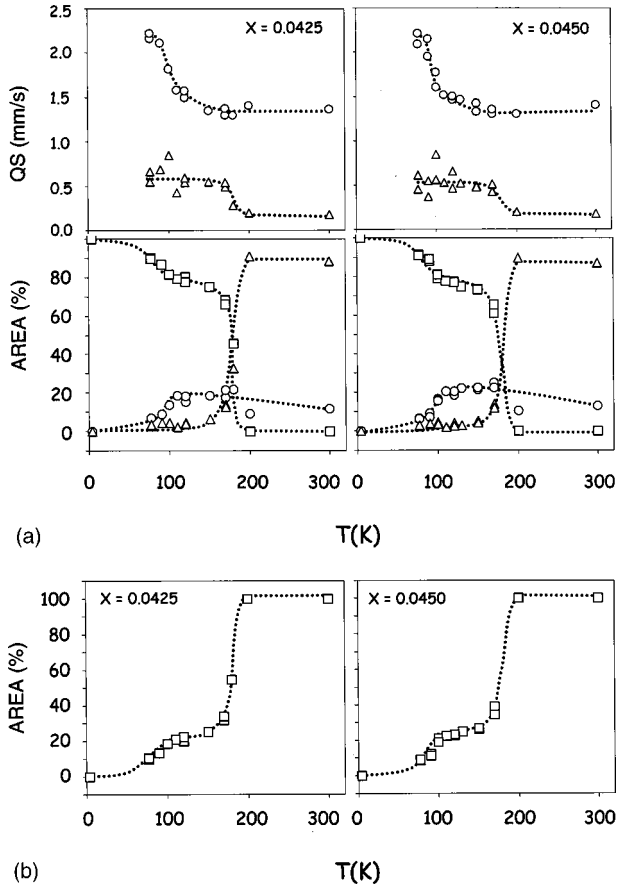


FIG. 5. (a) Quadrupole splitting (QS) and the corresponding area ratio (%) as a function of temperature obtained from the Mössbauer spectra for $x=0.0425$ and 0.0450 samples. Here (△) corresponds to the component with low QS and (○) corresponds to the component with high QS value. The data shown with (□) represent the magnetic contribution to the spectrum; (b) The paramagnetic contribution to the spectrum as a function of temperature. Note a significant contribution below $T_C$.

90% of the Mössbauer spectrum, and a weaker (10%) broad spectral feature with a lower hyperfine field. Before we proceed to discuss the fitting and the corresponding analysis of Mössbauer spectra, it is important to emphasize that the spectra for the two values of $x$ are similar whereas the two samples are in regions of entirely different electron transport regimes.

In order to obtain the hyperfine interaction parameters for the temperature range 77–170 K, where the paramagnetic-like and ferromagnetic contributions appear to coexist, we attempted three different fitting procedures:

(i) The first fitting procedure involved use of a unique, continuous and discrete distribution of static hyperfine fields. The objective here was to examine the quality of fitting achievable under the assumption that all the probe Fe atoms are in ferromagnetic state below the Curie temperature of the CMR and what, if any, can be learned from the evolution of the fitted hyperfine parameters with temperature. Under this procedure, the mean isomer shift $\langle IS\rangle$ is found to be characteristic of $Fe^{3+}$. Examples of distributions obtained at different temperatures are shown in Fig. 6. It is important to note the presence of two humps in the distributions. For $77<T<170\,K$, the position of the high-field peak shifts towards

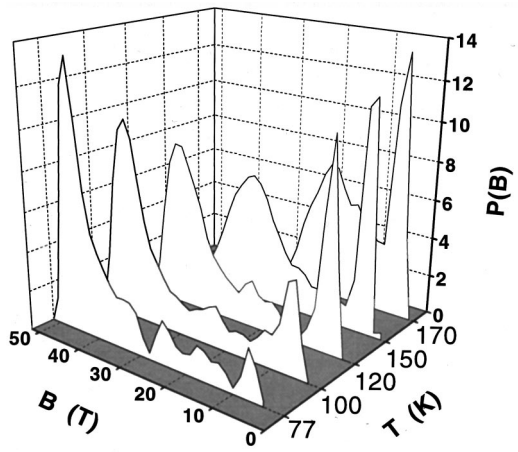


FIG. 6. Hyperfine field distributions as a function of the temperature: 170, 150, 120, 100, 77 K. $P(B)$ is a measure of the relative contribution of the component representing magnetic hyperfine field $B$ at temperature $T$ to the spectrum.

higher fields when the temperature decreases, whereas the low-field peak progressively diminishes although its position remains nearly temperature independent. If the apparent low-field contribution were truly ferromagnetic in origin, albeit with low mean field, one would have expected its position to shift to higher mean field with decreasing temperature, as observed for the high-field component. The fact that this shift is not seen strongly suggests that the apparent low-field contribution should actually be paramagnetic in nature with some quadrupole broadening. This motivated the next fitting procedure. Before presenting the same, it is useful to state that within the current procedure the average magnetic field increases when the temperature decreases, as shown in Fig. 7. The same characteristic evolution was found for $x=0.0425$ and 0.0450.

(ii) The second fitting procedure was based on a distribution of static hyperfine fields and two quadrupolar components, similar to those observed within the paramagnetic range ($T>T_C$). The use of the latter components was specifically motivated by the consideration that the paramagnetic contribution below $T_C$ may be emerging in the form of the residue of the same paramagnetic phase (with due temperature evolution), which is the main phase above $T_C$. In

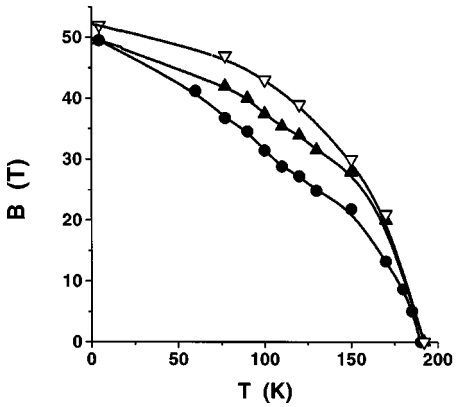


FIG. 7. Evolutions of the average $\langle B\rangle$ hyperfine field for $x=0.0425$ (●) and 0.045 (▲), and of the average hyperfine field without consideration of the paramagnetic component (▽).

this scheme, remarkably, the value of the smallest QS is seen to increase suddenly at 190 K when the magnetic component appears [Fig. 5(a)]. The quadrupolar splitting of the second doublet also increases but only when the temperature is lowered below 120 K. Interestingly, the area ratio evolution observed in Fig. 5(a) shows that it is the component with the low QS which first encounters a paramagnetic-magnetic transition around 190 K.

Remembering that the QS parameter, which effectively measures the electric-field gradient at the Fe site, is a sensitive reflection of local lattice symmetry; the observed evolutions could be related to some structural transformations within the residual paramagnetic region. We will discuss this issue further in the course of discussion based on the analysis of suggested models for the so-called ferromagnetic metallic state. Under this fitting procedure as well, the total magnetic contribution to the spectrum is seen to enhance with the lowering of temperature, as expected.

(iii) Finally, the series of these spectra were also analyzed using a distribution of static hyperfine magnetic fields in addition to a quadrupolar component accounting for the low-field contribution. Use of this third procedure was motivated by the thinking that the paramagneticlike phase seen below $T_C$ could be characteristically different as compared to the paramagnetic phase above $T_C$, and as such, the search for the fitting parameters need not necessarily revolve around the parameters for the phase above $T_C$, as was done in the second procedure. In fact, Uehara *et al.* suggest that in LCMO the nonmagnetic component below $T_C$ is in the form of 50:50 charge ordered state, with charge defects incorporated to compensate for the mean $Mn^{3+}/Mn^{4+}$ ratio.

With this third procedure, the quadrupolar component exhibits broad lines, which strongly increase when the temperature decreases, and progressively split into a broad magnetic feature. The evolution of the mean value of the hyperfine field due to the magnetic contribution is compared to previous ones in Fig. 7.

Mössbauer spectra were also registered at 100 and 8 K under an external field of 6 T applied in the direction of the $^{57}Co$ beam line in order to reduce the thermal fluctuations of the Fe magnetic moments (Fig. 8). At 100 K, the intensities of the intermediate lines 2 and 5 are seen to diminish in the presence of field (compared with the no-field 100-K data in Fig. 3), indicating that the iron moments become aligned along the external field. The distribution of effective hyperfine field is also shifted towards high fields, as illustrated in Fig. 9. At 8 K, the disappearance of the intermediate lines is complete and one clearly observes three well-defined magnetic components (Fig. 8). Let us examine the effective-field values, which result from the vector sum of the hyperfine field and the applied field. The effective fields of the two main components of 59(1) T and 54(1) T are consistent with a perfect antiparallel alignment of $Fe^{3+}$ magnetic moments with the external field, since it is well known that the sign of hyperfine field in $Fe^{3+}$ oxide systems is negative. On the contrary, the last component exhibits an effective field of 39(1) T which is lower than the hyperfine field and would suggest that the $Fe^{3+}$ moments are oriented parallel to the external field.

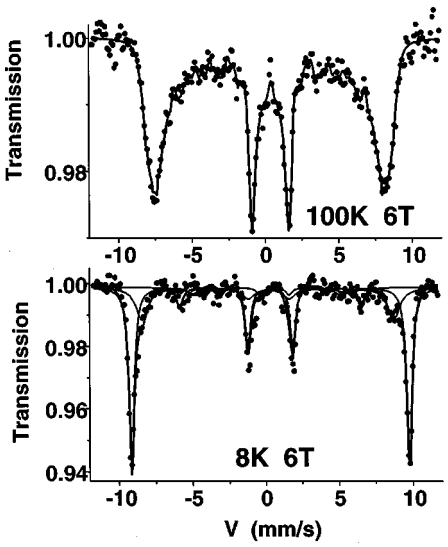


FIG. 8. Mössbauer spectra for $x=0.045$ registered under a longitudinal external applied field of 6 T at 100 and 8 K.

## IV. DISCUSSION

In a previous paper (Ref. 19), we have shown that the iron atoms do not directly contribute to the carrier transport in LCMO but that they drastically affect the transport properties with the creation of localization centers for the charge carriers. Above a well-defined threshold of iron concentration ($x \geqslant 0.04$) the distance between iron atoms becomes smaller than three lattice units, and the hopping of the quasiparticles associated with the double exchange process encounters the hindrance of the iron networks. This produces sudden modifications of the transport properties. However, since the ferromagnetic coupling appears for temperatures different than the peak temperatures $T_p$, we did not find a direct correlation between the transport and the macroscopic magnetism properties. Interestingly, a second hump on the low-temperature side appears in the CMR vs $T$ dependence (Fig. 1) for Fe concentrations above the threshold value of $x \sim 0.0425$, at which significant changes in the transport also occur.

While x-ray-diffraction analysis reveals the existence of only one phase with no perceptible modification with iron incorporation, our Mössbauer spectra indicate that all $Fe^{3+}$

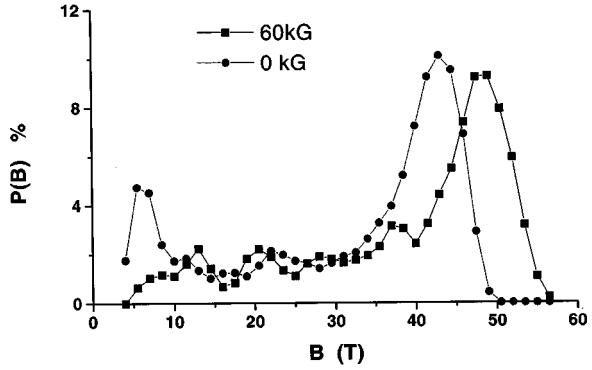


FIG. 9. Hyperfine field distribution $P(B)$ corresponding to the Mössbauer spectra registered at 100 K without (●) and with (■) an applied external field of 6 T.

cations do not experience similar hyperfine interaction environments. Pissas *et al.* have also found indications of the presence of two phases in their Mössbauer spectra.[17] The first phase corresponds to the ferromagnetic part of the spectrum and the second to the paramagnetic (or relaxed) part of the spectrum. In fact our data show that the ferromagnetic metallic state in these systems is intrinsically inhomogeneous, with paramagnetic contributions persisting down to temperatures much lower than the Curie temperature. This information revealed from magnetic relaxation effects should also reflect on the nature of carrier dynamics in this unusual metal in its ferromagnetic state. Our results support the view that different $Mn^{3+}/Mn^{4+}$ environments in terms of their dynamics and couplings are intrinsically formed in manganites. The various couplings between Fe and Mn then induce different electronic relaxation times for the Fe atoms. Also, in the case of large distances between two iron atoms, the effective Fe-Fe exchange energy is weak and, because of the fast electronic relaxation, it is necessary to cool down the sample to very low temperature to observe full magnetic order. This intrinsic inhomogeneity should translate into a distribution of magnetoresistance temperatures. Let us see whether this scenario can explain the second hump in the CMR curve and a broad rising CMR at lower temperatures for higher Fe concentrations. In this context it is useful to point out the observations of De Teresa *et al.*[27] who detected spontaneous formation of localized magnetic clusters of size between 0.8 and 2 nm in diameter above $T_C$ and showed that application of a magnetic field causes growth of the clusters but decrease in their number. These authors attributed the occurrence of CMR effect near $T_C$ to the existence of such small magnetic polarons (resulting from short-range ferromagnetic interactions) and their growth under magnetic field leading to percolation. Given our mean Fe-Fe separation of three lattice units or $\sim$1.2 nm at the threshold when sudden changes in the transport features are seen (which is close to the polaron size regime of De Teresa *et al.*[27]), we can see that regions where the Fe-Fe separation is higher than the polaron size would begin to percolate leading to the first normal peak in the CMR. For other regions, lower the temperature more will be the number of local regions converted by the magnetic field into ferromagnetic metallic state and therefore larger will be the MR, as seen. Pissas *et al.*[17] did not see these different temperatures and two humps perhaps because the iron concentration in their samples was too low ($x<0.02$). Indeed, in our study as well, the CMR curves did not clearly display a second hump when $x<0.0425$. This also eliminates the possibility of grain-boundary phenomena as being the major cause of the peculiar structure in MR vs $T$ dependence seen in our samples at larger Fe concentrations, since we did not see any differences in the grain structure for the concentrations of 0.04 and 0.045.

Our observation of the nonferromagnetic Fe below $T_C$ [Fig. 5(b)] almost down to 77 K is interesting, and should find its origin in the unusual and probably two-phase nature of the manganite system. Booth *et al.*[28] employed x-ray-absorption fine-structure measurements to obtain the distortions of Mn-O bond length and thereby the temperature evolution of the delocalized hole concentration. They found that the distortions are present even at temperatures much below $T_C$, implying the presence of a significant concentration of localized holes in the so-called ferromagnetic regime. Persistence of lattice distortions at temperatures much below $T_C$ was also found to be necessary for the theoretical explanation of the unusual transport behavior in terms of the double exchange and Jahn-Teller coupling. Chechersky *et al.*[29] performed temperature- and field-dependent Mössbauer study of $La_{0.8}Ca_{0.2}MnO_3$ compound by replacing a few parts per million of Mn with $Co^{57}$. They found that disappearance of ferromagnetic species occurs progressively starting at $T/T_C > 0.65$, which is much below $T_C$. They suggested a gradual crumbling of ferromagnetic order into small superparamagnetic clusters as $T_C$ is approached from below. Jaime *et al.*[9] have analyzed the temperature dependence of resistivity by using an effective-medium approach for a two-component system. They found that a low percolation threshold seems to explain the data well, and argued that the metal regions with sticklike or stripelike shape could yield such a low threshold. Similarly, studies of the decrease of the density of states from photoemission studies,[30–32] density of holes from the Hall effect,[33] the decrease in the height of the pair-distribution function peak,[34] and the development of quasi-elastic neutron-scattering component with temperature[35] collectively suggest that changes occur in the LCMO system over a span of temperatures below $T_C$ and not exactly at $T_C$. All these results and analyses imply that even much below $T_C$ the state of manganite could have two components: one ferromagnetic metal and another paramagneticlike insulator. Uehara *et al.*[7] suggest that the latter is in fact the 50:50 charge ordered state, but with charge defects to accommodate charge neutrality. Thus the nonmagnetic Fe reflected in our spectra could be the iron within such a paramagneticlike component itself or that in a small cluster which undergoes rapid superparamagnetic relaxation. Indeed, small clusters display paramagneticlike Mössbauer spectra due to fast fluctuation of their magnetic moment. At lower temperatures, the fluctuation frequency decreases and a magnetic hyperfine splitting occurs for frequencies smaller than the Larmor frequency of the $^{57}$Fe magnetic moment ($5\times10^8\ s^{-1}$). The progressive evolution observed in the temperature interval 77–170 K could be explained by a distribution of sizes of these clusters or by different neighboring configurations. Such experimental features agree well with those observed by Pissas *et al.*[17]

It is now interesting to examine if Mössbauer spectrometry can confirm some simultaneous structural changes near the transition temperature $T_C$. In Ref. 27 lattice distortions produced by the polaronic effect were detected by measuring the volume thermal expansion between 1.8 $T_C$ and $T_C$. At $T_C$ the lattice distortion was seen to disappear due to the delocalization of the carriers at the insulator-metal transition. Recently, it has been shown by neutron diffraction on $La_{0.65}Ca_{0.35}MnO_3$ that around the Curie temperature an anomalous change of the volume as well as modifications of oxygen-manganese distances take place while the structure remains orthorhombic whatever the temperature.[29] X-ray-absorption fine-structure (XAFS) measurements have also shown a rapid change in the Debye-Waller broadening parameter $\sigma^2$ for the Mn-O and Mn-Mn atom pairs near $T_C$.[22] Another study using high-resolution synchrotron x-ray powder diffraction on $La_{0.75}Ca_{0.25}MnO_3$ has revealed an abrupt decrease of all lattice parameters and a volume discontinuity

below the Curie temperature.[25] All these results are in agreement with the theoretical predictions of Millis *et al.*[13] and confirm that the dynamic Jahn-Teller distortion has to be taken into account for the understanding of the microscopic origin of the CMR effect. Another publication concerning the same system and reporting thermoelectric power and electrical resistivity measurements supports the theory of an electrical conduction dominated by polaron effects having both lattice and magnetic character.[20]

In our samples, it is clear that the temperature dependence of the quadrupolar splittings is rather unusual [Fig. 5(a)]. The enhancement of the quadrupolar splitting below 175 K for the most populated doublet and below 100 K for the second doublet reflects some local structural transformations. In fact, the interesting evolution of quadrupole splitting with temperature appears to find a natural explanation in the percolative picture of transport provided by Jaime *et al.*[9] In the region much above $T_C$ ($T_p$), the quadrupole splitting of the main fraction represents the paramagnetic state, which could have transient ferromagnetic fluctuations. As the para-ferro transition is approached from above $T_C$, the ferromagnetic clusters would tend to stabilize in space. Since within these clusters there are no or negligible Jahn-Teller distortions, formation of such stable clusters would cause changes in the strain distribution around them. In fact, the establishment of connectivity of ferromagnetic regions at the transition would change the shape function of the paramagnetic regions from a global three-dimensional form to more of a plateletlike configuration, especially if the clusters are sticklike or stripelike as suggested by Cheong *et al.*[36] and Jaime *et al.*[9] The change in the shape function should introduce further asymmetry in strain fields in the leftover paramagneticlike regions, causing enhancement of the splitting concurrently with the reduction of the paramagnetic component, as observed. As the temperature is reduced even further the shape asymmetry should grow further as reflected by a further gradual rise in the quadrupole splitting too. There is another interesting possibility that the sudden increase in the quadrupole splitting could be due to the fact that the paramagneticlike regions left in the ferromagnetic regime do not have the same character as the paramagnetic phase above $T_C$, but rather a charged ordered state (with charge defects) as proposed by Uehara *et al.*[7] in their phase separation scenario. However, between the fittings obtained by using the second and third procedures discussed earlier, the second one gave a better fit. Thus the former explanation in terms of changes in the shape function appears more reasonable.

We believe that the smaller ($<10\%$) component in the spectrum which corresponds to larger quadrupole splitting possibly represents the regions near grain boundaries in our polycrystalline samples. The large quadrupole splitting in this case can be attributed to the extended-defect-related strain fields. Also, the para-ferro transition in such regions would occur at lower temperature. The rise in the quadrupole splitting of this smaller fraction at about 120 K appears to be the signature of this temperature. It may be noted that in contrast to the changes in the main component near $T_C$, the changes near 120 K are over a broader temperature scale, which further supports that this small contribution originates from grain-boundary regions. In each case these lattice modifications which take place when magnetism appears support the existence of a strong coupling between the lattice and magnetism as proposed by Dai *et al.*[37]

Experiments performed under an applied external field confirm the existence of two different couplings. The fact that the moments of the major fraction of Fe atoms are essentially anti-parallel to the moments of Mn atoms shows that the Mn-O-Fe exchange is anti-ferromagnetic; apparently because no double exchange occurs between these two atoms and therefore the $t_{2g}$ superexchange dominates. However, we cannot exclude that iron atoms near grain boundaries behave differently as compared to the iron atoms embedded in ferromagnetic clusters due to the additional parameter of local strain variable. It seems that the small contribution of about 10% of Fe atoms aligning parallel to the external field and the Mn moments represent the grain-boundary region. Interestingly, the paramagneticlike spectral component which shows rise in the quadrupole splitting at lower temperature of 100 K is also about 10%, which could be attributed to the grain-boundary region.

## ACKNOWLEDGMENTS

This work was supported in part by the Indo-French Center for Promotion of Advanced Research (IFCPAR) under Contract No. 1208-1. One of us (S.B.O.) would like to thank Dr. T. Venkatesan for fruitful discussions. The authors would like to thank Druette Loïc for his help with the figures.

*Author to whom correspondence should be addressed. Electronic address: marest@cismsun.univ-lyonl.fr

[1] K. Chahara, T. Ohno, M. Kasai, and Y. Kosono, Appl. Phys. Lett. **63**, 1990 (1993).

[2] R. von Helmolt, J. Wecker, B. Holzapfel, L. Schultz, and K. Samwer, Phys. Rev. Lett. **71**, 2331 (1993).

[3] S. Jin, T. H. Tiefel, M. McCormack, R. A. Fastnacht, R. Ramesh, and L. H. Chen, Science **264**, 413 (1994).

[4] H. L. Ju, C. Kwon, Qi Li, R. L. Greene, and T. Venkatesan, Appl. Phys. Lett. **65**, 2108 (1994).

[5] S. Mori, C. H. Chen, and S.-W. Cheong, Nature (London) **392**, 473 (1998).

[6] Y. Murakami, J. P. Hill, D. Gibbs, M. Blume, I. Koyama, M. Tanaka, H. Kawata, T. Arima, Y. Tokura, K. Hirota, and Y. Endoh, Phys. Rev. Lett. **81**, 582 (1998).

[7] M. Uehara, S. Mori, C. H. Chen, and S.-W. Cheong, Nature (London) **399**, 560 (1999).

[8] A. Moreo, S. Yunoki, and E. Dagotto, Science **283**, 2034 (1999).

[9] M. Jaime, P. Lin, S. H. Chun, M. B. Salamon, P. Dorsey, and M. Rubinstein, Phys. Rev. B **60**, 1028 (1999).

[10] C. Zener, Phys. Rev. **82**, 403 (1951).

[11] J. B. Goodenough, Phys. Rev. **100**, 564 (1955); J. B. Goodenough and J.-S. Zhou, Nature (London) **386**, 229 (1997).

[12] P. G. de Gennes, Phys. Rev. **118**, 141 (1960).

[13] A. J. Millis, P. B. Littlewood, and B. I. Shraiman, Phys. Rev. Lett. **74**, 5144 (1995).

[14] J. Blasco, J. Garcia, J. M. Teresa, M. R. Ibarra, J. Perez, P. A. Algarabel, C. Marquina, and C. Ritter, Phys. Rev. B **55**, 8905 (1997).

[15] K. H. Ahn, X. W. Wu, K. Liu, and C. L. Chien, J. Appl. Phys. **15**,

5505 (1997).
[16] L. Righi, P. Gorria, M. Insauti, J. Gutierrez, and J. M. Barandiaran, J. Appl. Phys. **81**, 5767 (1997).
[17] M. Pissas, G. Kallias, E. Devlin, A. Simopoulos, and D. Niarchos, J. Appl. Phys. **81**, 5770 (1997).
[18] A. Simopoulos, M. Pissas, G. Kallias, E. Devlin, N. Moutis, I. Panagiotopoulos, D. Niarchos, C. Christides, and R. Sonntag, Phys. Rev. B **59**, 1263 (1999).
[19] S. B. Ogale, R. Skreekala, Ravi Bathe, S. K. Date, S. I. Patil, B. Hannoyer, F. Petit, and G. Marest, Phys. Rev. B **57**, 7841 (1998).
[20] M. F. Hundley, M. Hawley, R. H. Heffner, Q. X. Jia, J. J. Neumeier, J. Tesmer, J. D. Thompsen, and X. D. Wu, Appl. Phys. Lett. **67**, 860 (1995); M. Jaime, M. B. Salamon, M. Rubinstein, R. E. Treece, J. S. Horwitz, and D. B. Chrisey, Phys. Rev. B **54**, 11 914 (1996).
[21] A. P. Ramirez, S. W. Cheong, and P. Schiffer, J. Appl. Phys. **81**, 5337 (1997).
[22] C. H. Booth, F. Bridges, G. J. Snyder, and T. H. Geballe, Phys. Rev. B **54**, R15 606 (1996).
[23] P. Schiffer, A. P. Ramirez, W. Bao, and S.-W. Cheong, Phys. Rev. Lett. **75**, 3336 (1995).
[24] P. G. Radaelli, D. E. Cox, M. Marezio, S.-W. Cheong, P. E. Schiffer, and A. P. Ramirez, Phys. Rev. Lett. **75**, 4448 (1995).
[25] J. Teillet and F. Varret (unpublished).
[26] G. A. Sawatzky, F. Van der Woude, and A. H. Morrish, Phys. Rev. **187**, 747 (1969).
[27] J. M. De Teresa, M. R. Ibarra, P. A. Algarabel, C. Ritter, C. Marquina, J. Blasco, J. Garcia, A. del Moral, and Z. Arnold, Nature (London) **386**, 256 (1997).
[28] C. H. Booth, F. Bridges, G. H. Kwei, J. M. Lawrence, A. L. Cornelius, and J. J. Neumeier, Phys. Rev. Lett. **80**, 853 (1998).
[29] V. Chechersky, A. Nath, I. Issac, P. Franck, K. Ghosh, H. Ju, and R. L. Greene, Phys. Rev. B **59**, 497 (1999).
[30] D. N. McIlroy, J. Zhang, S.-H. Liou, and P. A. Dowben, Phys. Lett. A **207**, 367 (1995).
[31] J.-H. Park, C. T. Chen, S.-W. Cheong, W. Bao, G. Meigs, V. Chakarian, and Y. U. Idzerda, Phys. Rev. Lett. **76**, 4215 (1996).
[32] D. D. Sarma, N. Shanthi, S. R. Krishnakumar, T. Saitoh, T. Mizokawa, A. Sekiyama, K. Kobayashi, A. Fujimori, E. Weschke, R. Meier, G. Keindl, Y. Takeda, and M. Takano, Phys. Rev. B **53**, 6873 (1996).
[33] J. E. Nanez-Regueiro, D. Gupta, and A. M. Kadin, J. Appl. Phys. **79**, 5179 (1996).
[34] S. J. L. Billinge, R. G. Di Francesco, G. H. Kwei, J. J. Neumeier, and J. D. Thompson, Phys. Rev. Lett. **77**, 715 (1996).
[35] J. W. Lynn, R. W. Erwin, J. A. Borchers, Q. Huang, A. Santoro, J. L. Peng, and Z. Y. Li, Phys. Rev. Lett. **76**, 4046 (1996).
[36] S.-W. Cheong and C. H. Chen, in *Colossal Magneto-resistance, Charge Ordering and Related Properties of Manganese Oxides*, edited by C. N. R. Rao and B. Raveau (World Scientific, Singapore, 1998).
[37] P. Dai, J. Zhang, H. A. Mook, S.-H. Liou, P. A. Dowben, and E. W. Plummer, Phys. Rev. B **54**, R3694 (1996).